
FINITE EXPRESSION METHODS FOR DISCOVERING PHYSICAL LAWS FROM DATA

Zhongyi Jiang

Department of Mathematical Sciences
 Department of Computer and Information Sciences
 University of Delaware
 Newark, DE, USA
 jzy@udel.edu

Chunmei Wang

Department of Mathematics
 University of Florida
 Gainesville, FL, USA
 chunmei.wang@ufl.edu

Haizhao Yang*

Department of Mathematics
 Department of Computer Science
 University of Maryland College Park
 College Park, MD, USA
 hzyang@umd.edu

ABSTRACT

Nonlinear dynamics is a pervasive phenomenon observed in various scientific and engineering disciplines. However, uncovering analytical expressions that describe nonlinear dynamics from limited data remains a challenging and essential task. In this paper, we propose a new deep symbolic learning method called the “finite expression method” (FEX) to identify the governing equations within the space of functions containing a finite set of analytic expressions, based on observed dynamic data. The core idea is to leverage FEX to generate analytical expressions of the governing equations by learning the derivatives of partial differential equation (PDE) solutions using convolutions. Our numerical results demonstrate that FEX outperforms all existing methods (such as PDE-Net, SINDy, GP, and SPL) in terms of numerical performance across various problems, including time-dependent PDE problems and nonlinear dynamical systems with time-varying coefficients. Furthermore, the results highlight that FEX exhibits flexibility and expressive power in accurately approximating symbolic governing equations, while maintaining low memory and favorable time complexity.

Keywords Finite expression method · Symbolic machine learning · Deep reinforcement learning · Combinatorial optimization · Data-driven modeling

1 Introduction

Partial differential equations (PDEs) and dynamical systems play a vital role in describing the fundamental laws of physics in various scientific and engineering domains. However, understanding the underlying mechanisms of complex systems in modern applications, such as climate science, neuroscience, ecology, finance, and epidemiology, remains a challenge. Traditionally, the governing equations of these systems have been derived from empirical forms [1, 2]. In recent years, the rapid advancement of computational power and the availability of vast amounts of observational and stored data have opened up new opportunities for data-driven methodologies to establish physical laws [3, 4, 5, 6, 7, 8, 9, 10, 11, 12, 13, 14, 15, 16, 17, 18, 19]. These data-driven approaches provide an alternative means to uncover the governing equations by leveraging the rich information contained within the data. By combining advanced computational techniques with data observation and analysis, researchers can now explore and understand the complex behavior of these systems in a more comprehensive and insightful way.

In the realm of discovering physical laws through data-driven methods, numerous scientists have made significant contributions since the early works [3, 4]. Over the past decade, the remarkable progress in machine learning, data science, and computing power has facilitated several groundbreaking endeavors to unveil the governing equations of physical systems. When the underlying physical system is known beforehand, deep learning methods have been explored to enhance modeling accuracy by learning data-adaptive system parameters alongside the known equations [5, 6]. However, the more challenging task arises when attempting to identify the complete physical system solely from data, without any prior knowledge. One prevalent approach is to employ deep learning as a black-box regression tool for data-driven modeling and prediction [7, 8, 9, 10]. Although this approach allows for theoretical analysis and accuracy guarantees [20, 21], it falls short in terms of analytically identifying the governing equations and, consequently, lacks interpretability.

In recent years, symbolic regression has emerged as a promising methodology for analytically identifying governing equations from data, enabling improved interpretability [11, 12, 13, 14, 15, 16, 17, 18, 19]. One popular symbolic approach involves constructing a comprehensive dictionary of mathematical symbols and learning a sparse linear combination of these symbols to approximate the desired governing equation through a least squares problem. Notably, a groundbreaking model called SINDy (Sparse Identification of Nonlinear Dynamics) [13] has provided significant insights into addressing this challenge. SINDy employs a sequential threshold ridge regression (STRidge) algorithm to recursively determine the sparse solution from a predefined library of basis functions. However, the success of this sparsity-promoting approach heavily relies on a well-defined candidate function library, which requires prior knowledge of the system. Furthermore, it is limited by the fact that a linear combination of candidate functions may not be sufficient to capture complex mathematical expressions. When dealing with a massive library size, the sparsity constraint is empirically observed to fail, and the resulting high memory and computational costs become prohibitive, particularly in high-order and high-dimensional systems.

Another popular approach in symbolic regression involves designing symbolic neural networks, which generate complex mathematical expressions through the linear combination and multiplication of mathematical symbols. One notable method in this category is PDE-Net [22, 23]. The capacity of symbolic neural networks to generate desired governing equations is determined by the depth and width of the network. The network depth plays a crucial role in capturing the nonlinearity of governing equations and needs to be sufficiently large to uncover highly nonlinear relationships. However, this poses a challenging optimization problem for symbolic neural networks, leading to reduced effectiveness of the approach. Moreover, the symbolic neural networks employed in PDE-Net are limited to representing polynomials of mathematical operators without considering time-varying coefficients. This restriction confines its applicability to a specific class of physical laws, limiting its usefulness in scenarios where time-varying coefficients are essential.

Symbolic regression methods, such as genetic algorithms (GA) [24] and genetic programming (GP) [25], have been recently employed for discovering governing equations. GP, in particular, has been proposed to identify approximate governing equations [26]. The underlying concept of GP involves evolving mathematical expressions to better fit given data, drawing inspiration from Darwin's theory of evolution. Unlike GA, which represents chromosomes as strings of binary digits, GP represents mathematical expressions as tree-structured chromosomes consisting of nodes and terminals. During the training process, GP employs random crossover and mutation operations on mathematical expressions to evolve generations of expressions. However, due to the discrete nature of the optimization process in GP, there is a lack of continuous optimization for fine-tuning parameters. As a result, GP faces difficulties in providing highly accurate mathematical expressions, even for cases involving constant coefficients.

Another method for identifying mathematical expressions, including governing equations, is based on reinforcement learning (RL) [27, 28, 29]. RL approaches have been applied to various tasks, with identifying governing equations being one specific application. However, the existing literature predominantly focuses on numerical tests involving polynomial functions or simple dynamical systems characterized by constant coefficients. A recent method called Symbolic Physics Learner (SPL) [28] has introduced the use of Monte Carlo tree search (MCTS), a popular tool in RL, for discovering governing equations. SPL formulates the problem of symbolic regression within the framework of MCTS, where mathematical expressions containing operators and operands are generated concurrently by an agent. Only expressions yielding higher rewards are retained to update the agent. However, due to the simultaneous selection of operators and operands, SPL requires a large pool of candidate operators and operands. During its optimization process, SPL selects operands separately, resulting in the need for a large tree structure to represent the true expression. Consequently, solving the expression optimization problem becomes challenging.

In our paper, we extend the newly developed deep symbolic method [29], called the finite expression method (FEX), to identify the governing equations in the function space of mathematical expressions generated by binary expression trees with a fixed number of operators. The original FEX method [29] was proposed to identify the solutions of high-dimensional partial differential equations, where there is no learning mechanism to choose derivatives to form governing equations. A naive application of the original FEX requires a large number of derivatives for multiple

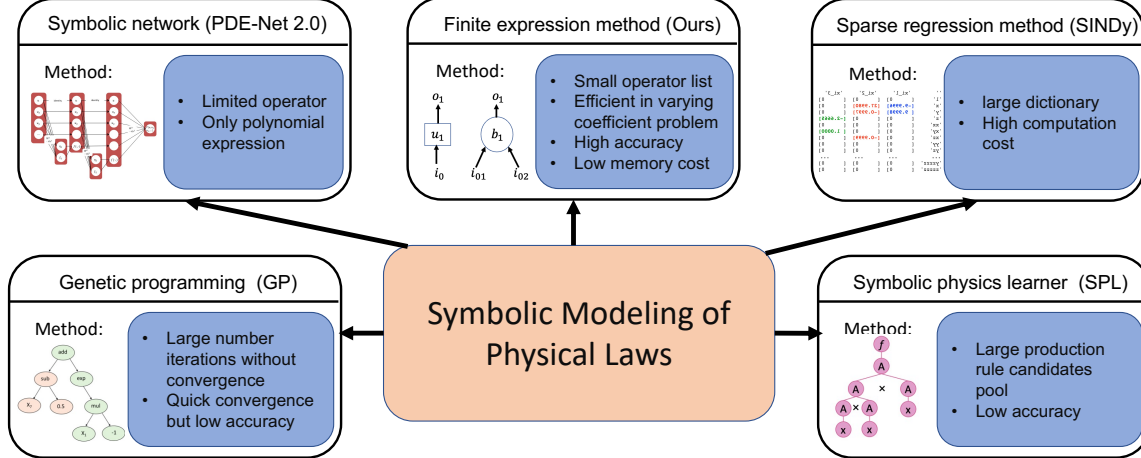


Figure 1: Overview of different symbolic methods for discovering governing equations from data.

variables in an operator list, making it very challenging to solve the expression optimization problem with the same issue as in SPL. In this paper, we adopt a data-driven way to learn the appropriate derivatives in a governing equation via continuous optimization, where identifying appropriate derivatives is equivalent to optimizing convolution kernels in convolution neural networks [22]. This continuous optimization significantly reduces the difficulty of learning a governing equation to learning a multivariate function, which can be solved by FEX efficiently. For example, learning $\frac{du}{dt} + u \frac{du}{dx} = 0$ is equivalent to learning a polynomial $ax + buy$ in x , u , and y , where a and b are convolution operators to implement derivatives (i.e., a matrix-vector multiplication).

In short summary, our new FEX defines a compact tree structure for all operands, and each leaf unary operator takes a linear combination of all operands with distinct parameters as input (e.g., trainable convolution parameters to learn function derivatives). This design reduces the complexity of the optimization problem, offering a more tractable solution compared to SPL, since our learning agent only needs to focus on operator sequence selection and learns the operands selection in a data-driven way via continuous optimization. Thus, our FEX significantly reduces the complexity of the expression optimization problem and extends the application range of the RL-based symbolic regression method to the discovery of PDE with varying coefficients.

Compared to other symbolic approaches, our new FEX for discovering physical laws enjoys the following advantages (summarized in Fig. 1): (1) Binary expression trees in FEX can generate a large class of mathematical expressions from a small number of operator list, avoiding the requirement of a large dictionary of symbols [13, 16] or a large symbolic neural network [22, 23]; (2) When learning simple equations with constant coefficients, FEX outperforms existing methods with a higher accuracy [13, 16, 22, 23, 26]; (3) FEX can effectively discover highly nonlinear governing equations with varying coefficients while baseline symbolic approaches fail [13, 16, 22, 23, 26]; and (4) The problem of searching for an appropriate mathematical expression is reformulated into a reinforcement learning (RL) problem, where the effective optimization algorithms are applicable with a high efficiency in memory cost. Therefore, FEX has the potential capacity to discover complex systems.

2 FEX Methodology

In this section, we will first review the convolutional filter method proposed in [22] to compute derivatives and then review the FEX method proposed in [29] for solving PDEs. Finally, we will propose a new FEX method for learning the symbolic governing equations.

2.1 Schemes for Computing Derivatives

Computing derivatives numerically is essential in solving differential equations. We shall first review the convolution filter method to compute derivatives [22]. A profound relationship between convolutions and differentiations can be found in [30, 31], where the connection between the order of sum rules of filters and the order of differential operators was discussed. To be precise, the definition of convolution operation on an image f follows the convention of deep

learning as follows

$$(f \otimes q)[l_1, l_2] := \sum_{k_1, k_2} q[k_1, k_2] f[l_1 + k_1, l_2 + k_2],$$

where \otimes is the circular convolution and q is a convolutional filter. This is essentially a correlation instead of a convolution in mathematics. For example, when the size of the filter is 5×5 , the initial values of the convolution kernels are

$$q_{01} = \begin{pmatrix} 0 & 0 & 0 & 0 & 0 \\ 0 & 0 & 0 & 0 & 0 \\ 0 & 0 & -3 & 4 & -1 \\ 0 & 0 & 0 & 0 & 0 \\ 0 & 0 & 0 & 0 & 0 \end{pmatrix}, \quad q_{02} = \begin{pmatrix} 0 & 0 & 0 & 0 & 0 \\ 0 & 0 & 0 & 0 & 0 \\ 0 & 1 & -2 & 1 & 0 \\ 0 & 0 & 0 & 0 & 0 \\ 0 & 0 & 0 & 0 & 0 \end{pmatrix}.$$

We compute $u_{01} = q_{01} \otimes u$, $u_{02} = q_{02} \otimes u$, where $u_{01} = \frac{\partial u}{\partial x}$, $u_{02} = \frac{\partial^2 u}{\partial x^2}$, and \otimes represents the convolutional operation.

2.2 Finite Expression Methods for Discovering Physical Laws

The finite expression method first proposed by Liang and Yang [29] is a deep reinforcement learning method to seek approximate solutions of PDEs in the space of functions composed of finitely many analytic expressions. [29] indicates that FEX can achieve high and even machine accuracy with a memory complexity polynomial in the problem dimension and an amenable time complexity. In this paper, we shall employ the idea of FEX to learn the symbolic governing equations. The architecture of our FEX is illustrated in Fig. 3. Compared with [29], we would like to emphasize that the settings are totally different. Figure 3 in [29] chooses derivative operators during discrete optimization of the operator list in the computational tree. However, we compute derivatives in advance and choose them by continuous optimization. In our FEX method, we first find a mathematical expression introduced in Section 2.2.1. Next, our combinatorial optimization (CO) is formulated in terms of the parameter and operator selection to seek the expression that approximates the governing equation. Reinforcement learning (RL) is used to select operators. The functional \mathcal{L} associated with the solutions of the PDEs or the dynamic systems acts as the environment to give the reward signal and provides the operator sequence to generate a reward. This reward guides the controller for better performance.

2.2.1 Function spaces in FEX

We first review the definition of mathematical expression proposed in [29] and then define finite expression methods for discovering physical laws.

DEFINITION 1 (Mathematical expression). [29] A *mathematical expression* is a valid function formulated by a combination of symbols that is well-formed by syntax and rules. The symbols consist of operands (variables and numbers), operators (e.g. "+", "-", integral, derivative), brackets, and punctuation.

DEFINITION 2 (Finite expression methods for discovering physical laws). The finite expression method is a methodology to learn a symbolic governing equation by seeking a finite expression to approximate the target equation.

2.2.2 Identifying governing equation expressions in FEX

A problem-dependent functional $\mathcal{L} : \mathbb{S} \rightarrow \mathbb{R}$ is associated with an unknown PDE or dynamic system, where \mathbb{S} is a function space and the minimizer of \mathcal{L} is the desired governing equation in \mathbb{S} to approximate the unknown PDE or dynamic system. When the number of operators k is given, the problem of learning a finite expression equation is formulated as a CO over \mathbb{S}_k via

$$\min \{\mathcal{L}(u) \mid u \in \mathbb{S}_k\}.$$

2.2.3 Binary trees in FEX

A well-defined binary tree \mathcal{T} can be used to formulate a finite expression as shown in Fig. 2. The order to traverse the tree is based on the operator sequence e consisting of tree nodes selected from the operator set. In FEX, tree input is a d -dimensional variable \mathbf{x} (see Fig. 3b). The unary operator linked to \mathbf{x} is applied to each entry of \mathbf{x} . The d -dimensional vector is mapped by a linear transformation from \mathbb{R}^d to \mathbb{R}^1 . All the parameters in these linear transforms will be trained and denoted by θ as the set of *learnable parameters* in FEX. Therefore, a finite expression is denoted by $u(\mathbf{x}; \mathcal{T}, e, \theta)$ as a function in \mathbf{x} . Given a fixed \mathcal{T} , the number of operators is fixed as $k_{\mathcal{T}}$. In FEX, $\mathbb{S}_{k_{\mathcal{T}}} = \{u_t(\mathbf{x}; \mathcal{T}, e, \theta) \mid e, \theta\}$ is the function space to identify the governing equation.

The design of the binary tree is demonstrated in Fig. 2. Each tree node is either a binary operator or a unary operator that is selected from the binary or unary set. The binary set could be $\mathbb{B} := \{+, -, \times, \dots\}$. Denote the identity map by

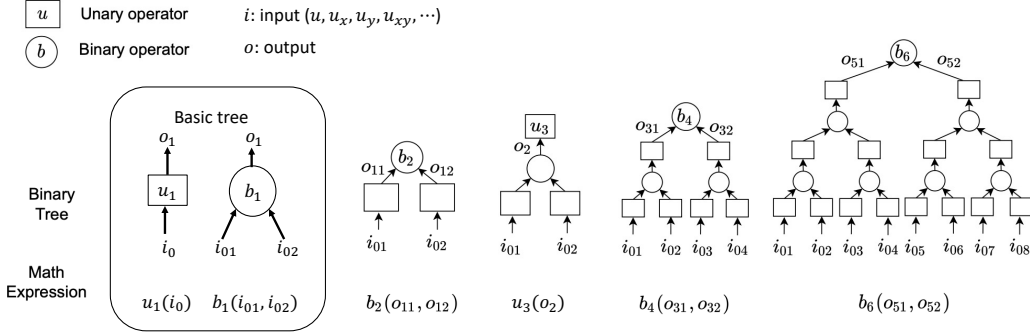


Figure 2: Computational rule of a binary tree. For a binary tree, the value of each node is either an unary or a binary operator. We define the computation flow of a basic tree that contains only one operator. For the binary tree with more than one layer, the computation is conducted by recursion.

Id. The unary set could be $\mathbb{U} := \left\{ \text{Id}, (\cdot)^2, (\cdot)^3, \sin, \exp, \log, \int \cdot dx_i, \frac{\partial}{\partial x_i}, \dots \right\}$. As an example, Fig. 3b shows a tree with 4 nodes and $e = (\text{Id}, \times, (\cdot)^2, (\cdot)^3)$.

2.2.4 Implementation of FEX

Given a fixed tree \mathcal{T} , FEX seeks the governing equation from the function space $\mathbb{S}_{k\mathcal{T}}$. The optimal mathematical expression is obtained via the following minimization problem

$$\min\{\mathcal{L}(u(\cdot; \mathcal{T}, e, \theta)) \mid e, \theta\}.$$

We introduce the framework of FEX, as demonstrated in Fig. 3 and Alg. 1. The basic idea is to find a good operator sequence e that approximately matches the true governing equation via minimizing the functional \mathcal{L} . In our framework, the searching loop (see Fig. 3 a) consists of four parts: 1) Reward computation (i.e., rewards of action in RL). A higher reward of an operator sequence e suggests a higher possibility to discover the governing equation. 2) Operator sequence generation (i.e., taking actions in RL). A controller is used to generate operator sequences. 3) Controller update (i.e., policy function update in RL). The controller is updated to increase the probability to generate a better operator sequence with higher rewards. The policy gradient method is used to update the controller to optimize the policy function in RL. 4) Candidate optimization (i.e., a non-greedy strategy). During the controller update process, FEX maintains a candidate pool to store operator sequences with a relatively high reward. After that, the parameter θ of each high-reward operator sequence is optimized to approximate the governing equation.

2.2.5 Reward computation

The reward of an operator sequence e guides the controller optimization to generate better operator sequences and maintains a good candidate pool of high scores. The reward of e , denoted by $R(e)$, is defined as follows

$$R(e) := (1 + L(e))^{-1},$$

where $L(e) = \min\{\mathcal{L}(u(\cdot; \mathcal{T}, e, \theta)) \mid \theta\}$. It is obvious $R(e) \in [0, 1]$. When $L(e)$ approaches 0, the equation expression approaches the true governing equation with the reward $R(e)$ approaching 1.

The first-order and second-order optimization algorithms are combined sequentially to accelerate the computation of $R(e)$. The first-order optimization algorithm (e.g., the stochastic gradient descent [32] and Adam [33]) might be time-consuming to optimize $L(e)$ since a large number of iterations is required. The second-order algorithm (e.g., Broyden-Fletcher-Goldfarb-Shanno method (BFGS) [34]) achieves faster convergence by the use of the Hessian matrix when an initial guess is good. In our method, the first-order algorithm is first used for T_1 steps to obtain a good initial guess, and the second-order algorithm is then applied for T_2 steps with the obtained good initial guess.

2.2.6 Operator sequence generation

The proposed controller acts as the policy function in RL to generate operator sequences e with high rewards. Denote by χ_Φ a controller with parameter Φ . χ_Φ is optimized by updating Φ to increase the probability for good operator sequences. The controller χ_Φ treats tree node values of \mathcal{T} as random variables, and outputs probability mass functions

Algorithm 1 FEX for Discovering Physical Laws

Input: The functional \mathcal{L} associated with derivatives of the solution of PDEs or dynamics system; A tree \mathcal{T} ; Searching loop iteration T ; Coarse-tune iteration T_1 with Adam; Coarse-tune iteration T_2 with BFGS; Fine-tune iteration T_3 with Adam; Pool size K ; Batch size N . **Output:** The governing equation $u(\mathbf{x}; \mathcal{T}, \hat{\mathbf{e}}, \hat{\theta})$.

Initialize agent χ for the tree \mathcal{T}

$\mathbb{P} \leftarrow \{\}$

for - from 1 to T **do**

 Sample N sequences $\{e^{(1)}, e^{(2)}, \dots, e^{(N)}\}$ from χ

for n from 1 to N **do**

 Optimize $\mathcal{L}(u(\mathbf{x}; \mathcal{T}, e^{(n)}, \theta))$ by coarse-tune with $T_1 + T_2$ iterations.

 Compute the reward $R(e^{(n)})$ of $e^{(2)}$

if $e^{(n)}$ belongs to the top- K of S **then**

$\mathbb{P}.\text{append}(e^{(n)})$

\mathbb{P} pops some e with the smallest reward when overloading

end if

end for

 Update χ using 2.2.7

end for

for e in \mathbb{P} **do**

 Fine-tune $\mathcal{L}(u(\mathbf{x}; \mathcal{T}, e, \theta))$ with T_3 iterations.

end for

$p_\Phi^1, p_\Phi^2, \dots, p_\Phi^k$ to identify their distributions, where k is the total number of nodes. Based on the corresponding probability mass functions, $e := (e_1, e_2, \dots, e_k)$ is the operator sequence sampled from χ_Φ (Fig. 3b).

2.2.7 Controller update

In our work, the controller χ_Φ is modeled as a neural network parameterized by Φ . We employ a policy-gradient-based updating method in RL to update the parameter Φ of the controller. The training objective of the controller is to maximize the expected reward of a sampled operator sequence e ; i.e.,

$$\mathcal{J}(\Phi) := \mathbb{E}_{e \sim \chi_\Phi} R(e),$$

where $e \sim \chi_\Phi$ means sampling an e from the controller χ_Φ , $R(e)$ is the reward of an sampled operator sequence e .

Denote the policy gradient by

$$\nabla_\Phi \mathcal{J}(\Phi) = \mathbb{E}_{e \sim \chi_\Phi} \left\{ R(e) \sum_{i=1}^k \nabla_\Phi \log (p_\Phi^i(e_i)) \right\},$$

where $p_\Phi^i(e_i)$ is the probability. For batch size N and $\{e^{(1)}, e^{(2)}, \dots, e^{(N)}\}$, we empirically compute the expectation of objective as follows

$$\nabla_\Phi \mathcal{J}(\Phi) \approx \frac{1}{N} \sum_{j=1}^N \left\{ R(e^{(j)}) \sum_{i=1}^k \nabla_\Phi \log (p_\Phi^i(e_i^{(j)})) \right\}.$$

The parameter Φ is updated via the gradient ascent with a learning rate η ; i.e.,

$$\Phi \leftarrow \Phi + \eta \nabla_\Phi \mathcal{J}(\Phi).$$

The objective function improves the average reward of N sampled sequences. We aim to find e with the best reward to discover governing equation. To increase the probability to obtain the best equation expression, we employ the objective function proposed in [35] and the risk-seeking policy gradient method proposed in [36] to seek the optimal operator sequence via

$$\mathcal{J}(\Phi) = \mathbb{E}_{e \sim \chi_\Phi} \{R(e) \mid R(e) \geq R_{\nu, \Phi}\}$$

where $R_{\nu, \Phi}$ represents the $(1 - \nu) \times 100\%$ -quantile of the reward distribution generated by χ_Φ and $\nu \in [0, 1]$. Therefore, the gradient computation becomes

$$\nabla_{\Phi} \mathcal{J}(\Phi) \approx \frac{1}{N} \sum_{j=1}^N \left\{ \left(R\left(\mathbf{e}^{(j)}\right) - \hat{R}_{\nu, \Phi} \right) \mathbf{1}_{\{R(\mathbf{e}^{(j)}) \geq \hat{R}_{\nu, \Phi}\}} \right. \\ \left. \sum_{i=1}^k \nabla_{\Phi} \log \left(p_{\Phi}^i\left(e_i^{(j)}\right) \right) \right\},$$

where $\mathbf{1}$ is an indicator function that returns 1 when the condition is satisfied otherwise 0, and $\hat{R}_{\nu, \Phi}$ is the $(1-\nu)$ -quantile of the reward $R\left(\mathbf{e}^{(i)}\right)$ for $i = 1, \dots, N$.

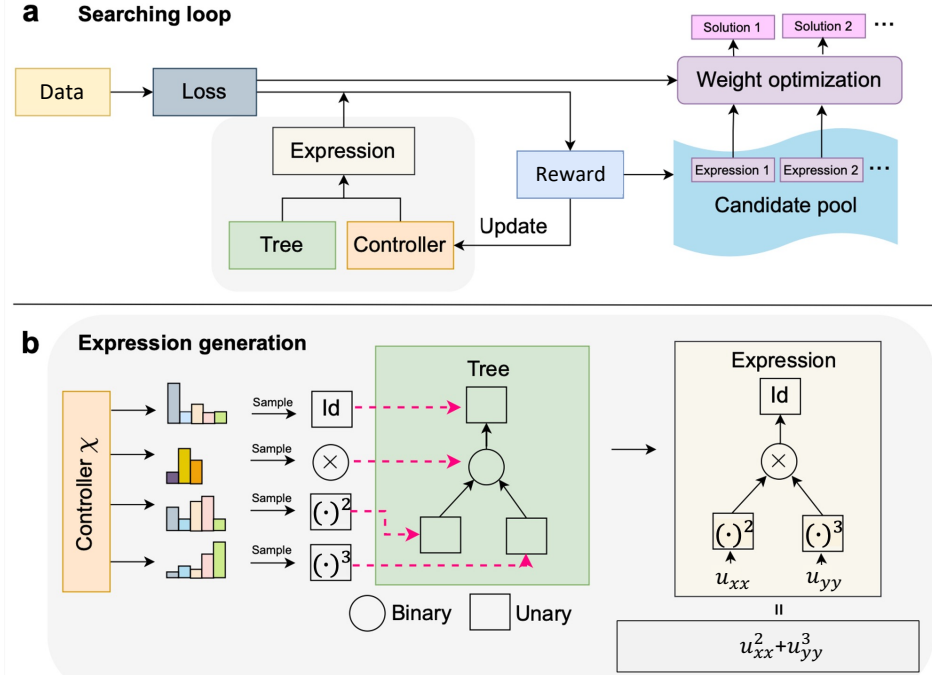


Figure 3: Representation of the components of our FEX. (a) The searching loop for the symbolic solution consists of expression generation, score computation, controller update, and candidate optimization. (b) Depiction of the expression generation with a binary tree and a controller χ .

3 Numerical Results

In this section, several numerical results are provided to demonstrate the accuracy and effectiveness of our FEX. We apply FEX to discover PDEs (e.g., Burgers' equation), nonlinear dynamical systems (e.g., 2D Hopf normal form), and nonlinear functions (e.g., Johnson-Mehl-Avrami-Kolmogorov equation) with possible time-varying coefficients. In comparison, PDE-Net 2.0 [22], SINDy [13], GP [25] and SPL [28] are applied for the test cases. All experiments are performed on a Macbook Pro with an Apple M1 Pro chip with 16 GB RAM. The goal of the numerical section is to demonstrate the following advantages of our FEX over these existing algorithms:

- For the simple problem, e.g., PDEs with constant coefficients in Section 3.1 and dynamical systems in a polynomial form in Section 3.3, all existing methods and FEX can discover the correct mathematical expression. However, our FEX admits higher accuracy and is memory-efficient.
- FEX can discover complicated nonlinear equations via SINDy and PDE-Net fail. See the example in Section 3.4.
- FEX can discover governing equations with time-varying coefficients while other symbolic approaches fail. See the example in Section 3.2.

- For each case, we present the training processes of three heuristic algorithms: GP, SPL, and FEX. Results show FEX gives more accuracy and robustness.

Experimental Settings: There are three main parts in the implementation of FEX. We will briefly describe the key numerical choices. (1) *Reward computation*. The reward is computed by the update of the functional with iteration numbers $T_1 = 500$ and $T_2 = 20$ using Adam and BFGS, respectively. (2) *Operator sequence generation*. The binary tree with 6 unary operators and 5 binary operators is used to generate mathematical expressions. The binary set is $\mathbb{B} = \{+, -, \times\}$ and the unary set is $\mathbb{U} = \{1, \text{Id}, (\cdot)^2, \dots\}$. A fully connected NN is used as a controller χ_Φ with a constant input. The output size of the controller NN is $n_1 + n_2$, where $n_1 = 5$ and $n_2 = 6$ are the numbers of binary and unary operators, respectively. (3) *Controller update*. The batch size for the policy gradient update is $N = 5000$ and the controller is trained for 500 iterations.

Given a series of measurements of some physical quantities $\{U(t, x, y) : t = t_0, t_1, \dots, (x, y) \in \Omega \subset \mathbb{R}^2\} \subset \mathbb{R}^d$ with d being the number of physical quantities of interest, we want to discover the governing PDE from the observed data $\{U(t, x, y)\}$. We assume that the observed data are associated with a PDE that takes the following general form:

$$U_t(t, x, y) = F(U, U_x, U_y, U_{xx}, U_{xy}, U_{yy}, \dots).$$

Here $U(t, \cdot) : \Omega \mapsto \mathbb{R}^d$, $F(U, U_x, U_y, U_{xx}, U_{xy}, U_{yy}, \dots) \in \mathbb{R}^d$, $(x, y) \in \Omega \subset \mathbb{R}^2$, $t \in [0, T]$. Our objective is to design a feed-forward NN by using FEX to discover the unknown PDE from its solution samples to reveal the analytic form of the response function F and the differential operators involved. In addition, we could conduct a long-term prediction of the dynamical behavior of the equation for any given initial condition.

In our numerical tests, we employ forward Euler to be the temporal discretization of the evolution PDE. Let $\tilde{U}(t + \delta t, \cdot)$ be the predicted value at time $t + \delta t$ based on $\tilde{U}(t, \cdot)$. We design an approximation framework as follows

$$\tilde{U}(t + \delta t, \cdot) \approx \tilde{U}(t, \cdot) + \delta t \cdot \text{FEXTree} \left(D_{00} \tilde{U}, D_{01} \tilde{U}, \dots \right),$$

where FEXTree is the binary tree \mathcal{T} described in Section 2.2.3, the operators D_{ij} are convolution operators with the underlying filters denoted by q_{ij} , i.e., $D_{ij}u = q_{ij} \otimes u$. Note that the operator $D_{ij}u$ approximates the differential operator $\frac{\partial^{i+j} u}{\partial^i x \partial^j y}$.

3.1 Burger's equation with constant coefficients

Burgers' equation is a fundamental PDE in many areas such as fluid mechanics and traffic flow modeling. It has a lot in common with the Navier-Stokes equation, e.g. the same type of advective nonlinearity and the presence of viscosity.

We consider Burgers' equation with periodic boundary condition on $\Omega = [0, 2\pi]^2$ [22]

$$\begin{cases} \frac{\partial u}{\partial t} &= -u \frac{\partial u}{\partial x} - v \frac{\partial u}{\partial y} + \nu \left(\frac{\partial^2 u}{\partial x^2} + \frac{\partial^2 u}{\partial y^2} \right), \\ \frac{\partial v}{\partial t} &= -u \frac{\partial v}{\partial x} - v \frac{\partial v}{\partial y} + \nu \left(\frac{\partial^2 v}{\partial x^2} + \frac{\partial^2 v}{\partial y^2} \right), \\ u|_{t=0} &= u_0(x, y), \\ v|_{t=0} &= v_0(x, y), \end{cases}$$

where $(t, x, y) \in [0, 4] \times \Omega$ and $\nu = 0.05$.

The training data is generated by a finite difference scheme on a 256×256 mesh. The second-order Runge-Kutta method with a time step size $\delta t = \frac{1}{1600}$ is employed for the temporal discretization in time. The second-order upwind scheme for ∇ and the central difference scheme for Δ are used for the spatial discretization. The initial values $u_0(x, y)$, $v_0(x, y)$ take the following form

$$w(x, y) = \frac{2w_0(x, y)}{\max_{x,y} |w_0|} + c,$$

where $w_0(x, y) = \sum_{|k|, |l| \leq 4} \lambda_{k,l} \cos(kx + ly) + \gamma_{k,l} \sin(kx + ly)$, $\lambda_{k,l}, \gamma_{k,l} \sim \mathcal{N}(0, 1)$, $c \sim \mathcal{U}(-2, 2)$. Here, $\mathcal{N}(0, 1)$, $\mathcal{U}(-2, 2)$ represent the standard normal distribution on $(0, 1)$ and the uniform distribution on $[-2, 2]$ respectively. We add noise to generate data as follows

$$\hat{u}(t, x, y) = u(t, x, y) + C \times MW,$$

where $M = \max_{x,y,t}\{u(t, x, y)\}$, $W \sim \mathcal{N}(0, 1)$ and $C = 0.001$ is the level of noise. Suppose we know a priori that the order of the underlying PDE is no more than 2. We shall use one FEXTree to approximate the right-hand side. Denote the FEXTree by Tree_u . Each δt forward of our FEX can be written as

$$\tilde{u}(t_{i+1}, \cdot) = \tilde{u}(t_i, \cdot) + \delta t \cdot \text{Tree}_u(D_{00}\tilde{u}, D_{01}\tilde{u}, \dots, D_{20}\tilde{v}),$$

where $\{D_{ij} : 0 \leq i + j \leq 2\}$ are convolution operators.

Table 1: Numerical Results of the Burger's equation term by term

Correct PDE	PDE-Net 2.0	SINDy	GP	SPL	FEX
$-uu_x$	$-1.00uu_x$	$0uu_x$	$-1.00uu_x$	$0uu_x$	$-1.00uu_x$
$-vu_y$	$-1.00vu_y$	$0vu_y$	$-1.00vu_y$	$-1.00vu_y$	$-1.00vu_y$
$0.05u_{xx}$	$0.0503u_{xx}$	$0.0832u_{xx}$	$0u_{xx}$	$0u_{xx}$	$0.0498u_{xx}$
$0.05u_{yy}$	$0.0503u_{yy}$	$0u_{yy}$	$0u_{yy}$	$0u_{yy}$	$0.0502u_{yy}$
	$5.98 \times 10^{-3}uv$	$5.55 \times 10^{-1}u^2u_x$	$7.6 \times 10^{-2}vu_{yy}$	u_x	$4.21 \times 10^{-4}u^2$
	$1.56 \times 10^{-3}u$	$-4.62 \times 10^{-1}u_yv^3$	$-1.7 \times 10^{-2}v^2u_{yy}$	0	$4 \times 10^{-4}u^2$
	$-8.02 \times 10^{-4}uu_y$	$-4.76e^{-1}u^2u_x$	0	0	$2 \times 10^{-4}u_x$
	$-6.78e^{-4}uu_xu_y$	$4.36 \times 10^{-2}uu_xu_{yy}$	0	0	$2 \times 10^{-4}u_{xy}$
	$-6.62 \times 10^{-4}v_x$	$-4.26 \times 10^{-2}v^2v_y$	0	0	$2 \times 10^{-4}v_x$
	-5.82×10^{-4}	$-3.5 \times 10^{-2}u_yvv_{yy}$	0	0	$2 \times 10^{-4}v_y$

Table 2: Absolute errors for the Burger's equation term by term

Correct PDE	PDE-Net 2.0	SINDy	GP	SPL	FEX
$-uu_x$	0	1	0	1	0
$-vu_y$	0	1	0	0	0
$0.05u_{xx}$	3×10^{-4}	3.3×10^{-3}	5×10^{-2}	5×10^{-2}	2×10^{-4}
$0.05u_{yy}$	3×10^{-4}	5×10^{-2}	5×10^{-2}	5×10^{-2}	2×10^{-4}
	5.98×10^{-3}	5.55×10^{-1}	7.6×10^{-2}	1	4.21×10^{-4}
	1.56×10^{-3}	4.62×10^{-1}	1.7×10^{-2}	0	4×10^{-4}
	8.02×10^{-4}	4.76×10^{-1}	0	0	2×10^{-4}
	6.78×10^{-4}	4.36×10^{-2}	0	0	2×10^{-4}
	6.62×10^{-4}	4.26×10^{-2}	0	0	2×10^{-4}
	5.82×10^{-4}	3.5×10^{-2}	0	0	2×10^{-4}

Table 3: Mean absolute error for the Burger's equation

	PDE-Net 2.0	SINDy	GP	SPL	FEX
Mean Absolute Error	1.086×10^{-3}	3.239×10^{-1}	1.93×10^{-2}	2.1×10^{-1}	2.021×10^{-4}

We demonstrate the accuracy of our FEX to recover the analytic form of the unknown PDE. The learnable parameter set θ in the linear transformation before each leaf node in the FEXTree and the operation set e chosen in each node provide attractive flexibility to obtain a desired governing equation. The 4 terms of the true equation and 6 more terms in descending coefficients learned by PDE-Net 2.0, SINDy, GP, and our FEX are listed in Table 1. We can see from Table 1 that FEX and PDE-Net can recover the governing equation more accurately than SINDy and GP. When we consider items other than the dominating 4 terms, FEX shows better numerical performance than PDE-Net, since it is hard to ignore the terms $5.98 \times 10^{-3}uv$ and $1.56 \times 10^{-3}u$ arising from PDE-Net.

In SINDy, there is a hyperparameter - $poly_{order}$ which determines the highest degree of polynomials in its dictionary. The default setup is $poly_{order} = 5$ in SINDy such that the size 6188 of the candidate function dictionary is too large to be run in Apple M1 Pro CPU with 16GB memory. In our FEX, we set $poly_{order} = 3$ with size 455 for the candidate function dictionary. We use the genetic programming-based symbolic regression as implemented in `gplearn` to provide the results of GP. The absolute error for each equation term and mean absolute error (MAE) shown in Table 2 and Table 3 are defined as follows

$$\text{Absolute Error} = |w_i - \tilde{w}_i| \text{ for } i = 1 \dots n,$$

$$\text{Mean Absolute Error} = \frac{\sum_{i=1}^n |w_i - \tilde{w}_i|}{n},$$

where w_i is the true coefficient for the corresponding term in the true equation, \tilde{w}_i is the corresponding numerical coefficient obtained from PDE-Net, SINDy, GP, SPL, and our FEX respectively, n is the total number of terms taken into consideration. We set $n = 10$ in this test including 4 dominating terms and 6 non-dominating terms.

Moreover, we also test the robustness of our method in different levels of noise. Results of FEX and PDE-Net can be seen in Table 4 and 5. FEX shows better robustness and accuracy in higher levels of noise than PDE-Net.

Table 4: Numerical Results of the Burger's equation by FEX with different levels of noise

Correct PDE	$C = 0.001$	$C = 0.005$	$C = 0.01$
$-uu_x$	-1.00 uu_x	-1.006 uu_x	-1.025 uu_x
$-vu_y$	-1.00 vu_y	-1.002 vu_y	-0.926 vu_y
0.05 u_{xx}	0.0498 u_{xx}	0.0534 u_{xx}	0.0617 u_{xx}
0.05 u_{yy}	0.0502 u_{yy}	0.0543 u_{yy}	0.0612 u_{yy}

Table 5: Numerical Results of the Burger's equation by PDE-Net with different levels of noise

Correct PDE	$C = 0.001$	$C = 0.005$	$C = 0.01$
$-uu_x$	-1.00 uu_x	-1.01 uu_x	-0.88 uu_x
$-vu_y$	-1.00 vu_y	-0.92 vu_y	-0.80 vu_y
0.05 u_{xx}	0.0503 u_{xx}	0.01 u_{xx}	0.01 u_{xx}
0.05 u_{yy}	0.0503 u_{yy}	0.02 u_{yy}	0.01 u_{yy}

Here, the training process of GP, SPL, and FEX is shown in Figure 4. For each method, we choose the worst and best result among 5 runs and present the mean and best result in Table 6.

Table 6: Best and mean MSE for the Burger's equation within 5 runs

	GP	SPL	FEX
Best	0.026	4.804	4.575×10^{-6}
Mean	0.159	9.975	2.134×10^{-4}

3.2 Burger's equation with varying coefficients

We consider a typical example of the Burger's equation with varying coefficients which seeks u such that

$$u_t(x, t) = a(t)uu_x + \nu u_{xx}, \quad \forall (x, t) \in [-8, 8] \times [0, 10],$$

$$u(x, 0) = \exp(-(x + 1)^2),$$

where $a(t) = 1 + \frac{1}{4} \sin t$ and $\nu = 0.1$. Burgers' equation can be solved numerically using `odeint` function in the SciPy package for 256 grid points and 256 time steps. The discrete Fourier transform (DFT) can be applied to evaluate spatial derivatives. We add 1% noise to generate data denoted by \tilde{u} . Suppose we know a priori that the derivatives \tilde{u}_x and \tilde{u}_{xx} . Our FEX can be written as

$$\tilde{u}(t_{i+1}, \cdot) = \tilde{u}(t_i, \cdot) + \delta t \cdot \text{Tree}_u(t, \tilde{u}, \tilde{u}_x, \tilde{u}_{xx}),$$

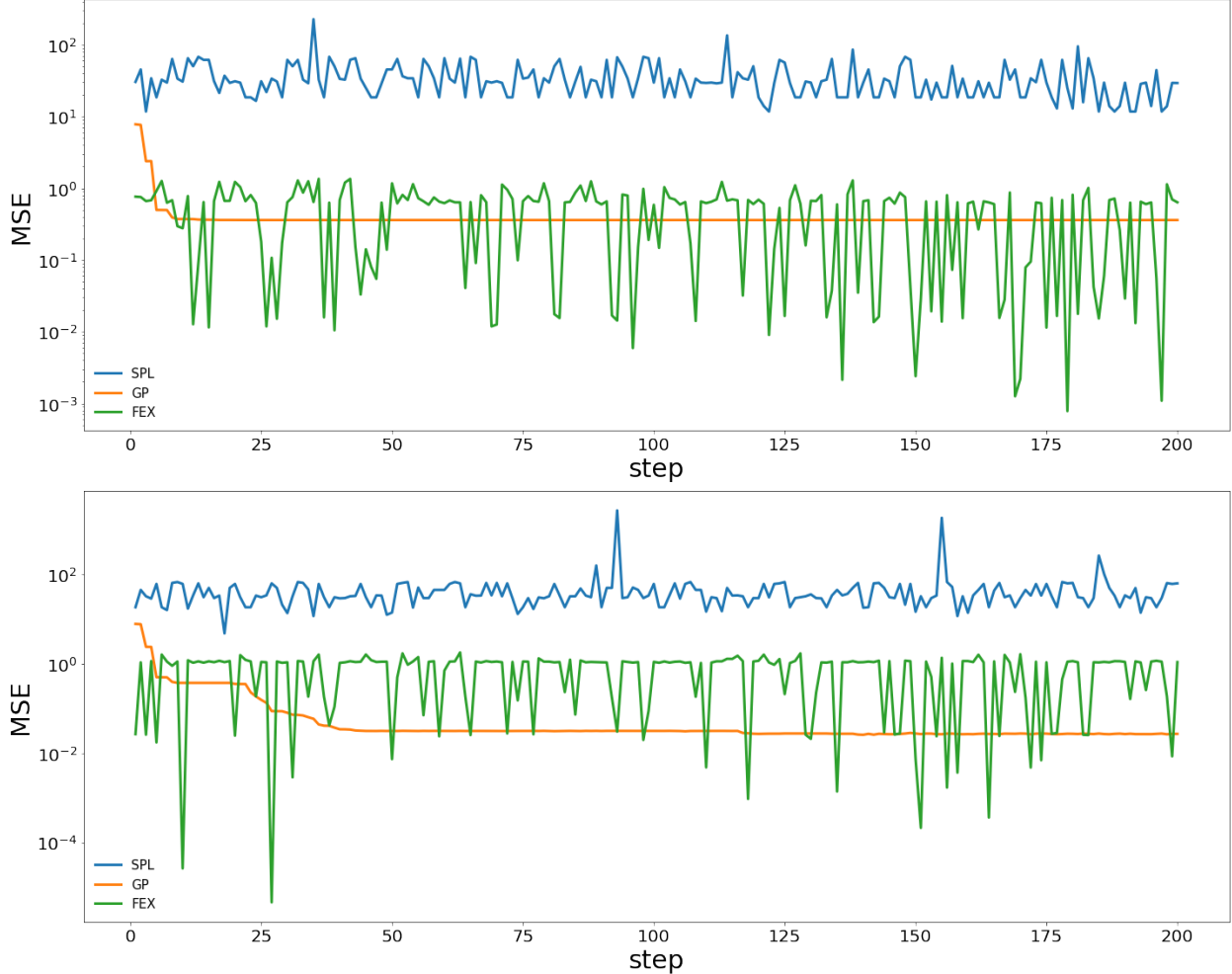


Figure 4: Up: Worst results among 5 runs of three methods. Down: Best results among 5 runs of three methods

where $t_{i+1} = t_i + \delta t$.

Numerical results learned by PDE-Net 2.0, SINDy, GP, SPL, and our FEX are illustrated in Table 7, which shows only our FEX can discover the varying coefficient of the nonlinear advection term while all other methods fail. Figure 5 demonstrates that our FEX method approximates both the constant coefficient and time-varying coefficient in the PDE with a small error. There has been some recent work that can identify the varying coefficient [37, 38, 39], where their numerical approximation is expressed numerically. However, our FEX method can effectively discover the governing equation in a symbolic/expression form with better interpretability.

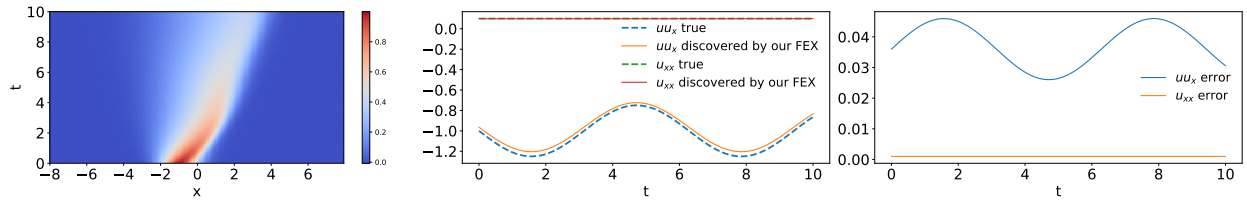


Figure 5: Left: Our numerical solution of Burger's equation with varying coefficients. Middle: Comparison of real and reconstructed coefficients of diffusion and advection term. Right: Absolute error.

Table 7: Comparison for the Burger's equation with varying coefficients.

Correct PDE	$u_t = -(1 + \sin(t)/4)uu_x + 0.1u_{xx}$
PDE-Net 2.0	$u_t = -0.780uu_x + 0.104u_{xx} - 0.326ux^3 + 0.316u^2u_x^2 - 0.225uu_x^2 + \dots$
SINDy	$u_t = -0.948uu_x - 0.100u_{xx} - 0.168u^2u_x - 0.087u_x^3 + 0.050uu_x^2 - 0.043u_x^2$
GP	$u_t = -1.011uu_x$
SPL	$u_t = -0.5491u_x$
FEX	$u_t = -0.964uu_x - 0.249 \sin(t)uu_x + 0.099u_{xx}$

Here, the training process of GP, SPL, and FEX is shown in Figure 6. For each method, we choose the worst and best result among 5 runs and present the mean and best result in Table 8.

Table 8: Best and mean MSE for the Burger's equation with varying coefficients among 5 runs

	GP	SPL	FEX
Best	8.940×10^{-4}	2.136×10^{-4}	5.698×10^{-7}
Mean	9.044×10^{-4}	1.805×10^{-3}	1.338×10^{-6}

3.3 2D Hopf normal form

In practice, many parametric systems in real applications may have bifurcations when parameters vary. The FEX algorithm is readily extended to encompass these important parameterized systems, e.g., allowing for the discovery of normal forms of \mathbf{x} associated with a bifurcation parameter μ . For example, the 2D Hopf normal form below is considered in [13]:

$$\begin{cases} \dot{x} = \mu x + \omega y - Ax(x^2 + y^2), \\ \dot{y} = -\omega x + \mu y - Ay(x^2 + y^2), \end{cases}$$

where $A = 1$ and $\omega = 1$. Experimental data are generated with the unstable $\mu = \{-0.15, -0.05\}$ and the stable $\mu = \{0.05, 0.15, 0.25, 0.35, 0.45, 0.55\}$.

Table 9: Comparison for the 2D Hopf normal form.

Correct equations	$\dot{x} = \mu x - y - x(x^2 + y^2)$ $\dot{y} = x + \mu y - y(x^2 + y^2)$
PDE-Net 2.0	$\dot{x} = 0.912\mu x - 0.998y - 0.930x^3 - 0.935xy^2$ $\dot{y} = 0.999x + 0.960\mu y - 0.979yx^2 - 0.930y^3$
SINDy	$\dot{x} = -0.993y$ $\dot{y} = 0.995x + 1.006\mu y - 1.006yx^2 - 1.008y^3$
GP	$\dot{x} = -y$ $\dot{y} = x$
SPL	$\dot{x} = -0.9391y$ $\dot{y} = x$
FEX	$\dot{x} = 0.984\mu x - 0.997y - 1.003x^3 - 1.004xy^2$ $\dot{y} = 0.996x + 1.014\mu y - 0.995yx^2 - 1.000y^3$



Figure 6: Up: Worst results among 5 runs of three methods. Down: Best results among 5 runs of three methods

We first demonstrate the ability of the trained FEX to recover the analytic form of the unknown dynamical system model for different μ 's with good accuracy. Numerical results by PDE-Net, SINDy, GP, SPL, and FEX are summarized in Table 9, which shows that PDE-Net and FEX can recover the desired governing equation, while SINDy, GP and SPL fail to find the correct equation. Furthermore, the 4 terms in the true equation and 6 more terms in descending coefficients generated by PDE-Net and FEX are shown in Table 10. We can see from Table 10 that our FEX outperforms PDE-Net 2.0 with better accuracy since the coefficients of the 6 more terms generated by our FEX are smaller than those generated by PDE-Net 2.0. We can see from Tables 11-12 that the absolute error per parameter and MAE of our FEX are smaller than those of PDE-Net 2.0. In addition, the visualization of the dynamics predicted by our FEX and the ground truth dynamics for $T \in [0, 2\pi]$ is demonstrated in Fig. 7, which shows that the governing equation learned by our FEX performs well in prediction.

Here, the training process of GP, SPL, and FEX is shown in Figure 8. For each method, we choose the worst and best result among 5 runs and present the mean and best result in Table 13.

3.4 Johnson-Mehl-Avrami-Kolmogorov nonlinear equation

We consider a nonlinear function in material science named Johnson-Mehl-Avrami-Kolmogorov equation (JMAK). Hereafter, we call JMAK Avrami equation. The Avrami equation describes the growth kinetics of phases in materials at a constant temperature. The Avrami equation is given by

$$y = 1 - \exp(-kt^n),$$

13

Table 10: Results of the 2D Hopf normal form per parameter

Correct PDE for \dot{x}	PDE-Net 2.0	FEX	Correct PDE for \dot{y}	PDE-Net 2.0	FEX
μx	$0.912\mu x$	$0.984\mu x$	x	$0.999x$	$0.996x$
$-y$	$-0.998y$	$-0.997y$	μy	$0.960\mu y$	$1.014\mu y$
$-x^3$	$-0.930x^3$	$-1.003x^3$	$-yx^2$	$-0.979yx^2$	$-0.995yx^2$
$-xy^2$	$-0.935xy^2$	$-1.004xy^2$	$-y^3$	$-0.930y^3$	$-1.000y^3$
	$-3.33 \times 10^{-1}xy^3$	$7.66 \times 10^{-2}y^3$		$-2.45 \times 10^{-1}\mu y^3$	$1.75 \times 10^{-2}\mu^3$
	$3.22 \times 10^{-1}\mu xy$	$6.35 \times 10^{-2}\mu y$		$1.25 \times 10^{-1}x^2y^2$	$-4.05 \times 10^{-3}\mu^2$
	$-3.20 \times 10^{-1}x^3y$	$2.16 \times 10^{-2}x\mu^2$		$1.20 \times 10^{-1}y^4$	$3.99 \times 10^{-3}\mu x^2$
	$3.09 \times 10^{-1}y^4$	$-5.41 \times 10^{-3}\mu^3$		$1.13 \times 10^{-1}\mu xy$	$2.80 \times 10^{-3}xy$
	$-3.04 \times 10^{-1}\mu y^2$	$2.70 \times 10^{-3}x$		$-1.09 \times 10^{-1}\mu xy^2$	$2.20 \times 10^{-3}y$
	$2.72 \times 10^{-1}x^2y^2$	$2.16 \times 10^{-3}x\mu^2$		$-1.03 \times 10^{-1}xy^4$	$1.64 \times 10^{-3}x^3$

Table 11: Absolute error of the 2D Hopf normal form per parameter

Correct PDE for \dot{x}	PDE-Net 2.0	FEX	Correct PDE for \dot{y}	PDE-Net 2.0	FEX
μx	8.80×10^{-2}	1.60×10^{-2}	x	1.00×10^{-3}	4.00×10^{-3}
$-y$	2.00×10^{-3}	3.00×10^{-3}	μy	4.00×10^{-2}	1.40×10^{-2}
$-x^3$	7.00×10^{-2}	3.00×10^{-3}	$-yx^2$	2.10×10^{-2}	5.00×10^{-3}
$-xy^2$	6.50×10^{-2}	4.00×10^{-3}	$-y^3$	7.00×10^{-2}	0
	$3.33 \times 10^{-1}xy^3$	$7.66 \times 10^{-2}y^3$		$2.45 \times 10^{-1}\mu y^3$	$1.75 \times 10^{-2}\mu^3$
	$3.22 \times 10^{-1}\mu xy$	$6.35 \times 10^{-2}\mu y$		$1.25 \times 10^{-1}x^2y^2$	$4.05 \times 10^{-3}\mu^2$
	$3.20 \times 10^{-1}x^3y$	$2.16 \times 10^{-2}x\mu^2$		$1.20 \times 10^{-1}y^4$	$3.99 \times 10^{-3}\mu x^2$
	$3.09 \times 10^{-1}y^4$	$5.41 \times 10^{-3}\mu^3$		$1.13 \times 10^{-1}\mu xy$	$2.80 \times 10^{-3}xy$
	$3.04 \times 10^{-1}\mu y^2$	$2.70 \times 10^{-3}x$		$1.09 \times 10^{-1}\mu xy^2$	$2.20 \times 10^{-3}y$
	$2.72 \times 10^{-1}x^2y^2$	$2.16 \times 10^{-3}x\mu^2$		$1.03 \times 10^{-1}xy^4$	$1.64 \times 10^{-3}x^3$

where the coefficients k and n vary in different environmental conditions.

In order to simulate the Avrami equation in different environmental conditions, we set $n = 2$ and append k as a variable in $y = f(k, t)$, and the data set is built up over multiple choices of $k = \{0.005, 0.01, 0.04, 0.1, 0.5, 0.8\}$. For each k , 20 samples are uniformly generated in $t \in [0, 1]$. The Avrami equation can be learned by our FEX as follows

$$\tilde{y} = \text{Tree}_y(t, k).$$

The numerical results learned by PDE-Net, SINDy, GP, SPL, and FEX are summarized in Table 14. We can see from Table 14 that our FEX can discover the Avrami equation with high accuracy while PDE-Net, GP, SINDy, and SPL fail.

Here, the training process of GP, SPL, and FEX is shown in Figure 9. For each method, we choose the worst and best result among 5 runs and present the mean and best result in Table 15.

4 Conclusion

In this paper, we propose a novel symbolic learning, named the ‘‘finite expression method’’ (FEX), to discover the governing equations from data. Our FEX can provide physically meaningful and interpretable formulas for physical laws compared to black-box deep learning methods. FEX only requires a small number of predefined operators to automatically generate a large class of mathematical formulas. As shown by extensive numerical tests, FEX enjoys favorable memory cost and can discover a large range of governing equations with better accuracy than other existing symbolic approaches such as PDE-Net, SINDy, SPL, and GP.

Table 12: Mean absolute error of the 2D Hopf normal form

	PDE-Net for \dot{x}	FEX for \dot{x}	PDE-Net for \dot{y}	FEX for \dot{x}
Mean Absolute Error	2.085×10^{-1}	1.977×10^{-2}	9.470×10^{-2}	5.518×10^{-3}

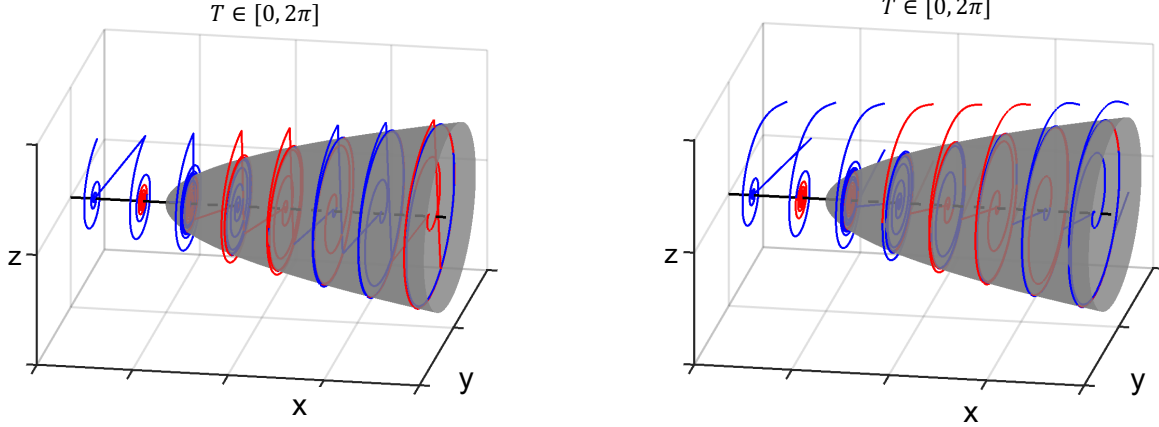


Figure 7: The visualization of the ground truth dynamics of the 2D Hopf normal form (left) and its prediction learned by FEX (right).

Acknowledgements

C. W. was partially supported by National Science Foundation under award DMS-2136380 and DMS-2206332. H. Y. was partially supported by the US National Science Foundation under award DMS-2244988, DMS-2206333, and the Office of Naval Research Award N00014-23-1-2007.

References

- [1] Messoud Efendiev. *Mathematical Modeling of Mitochondrial Swelling*. Springer, 2018.
- [2] Christopher Earls Brennen and Christopher E Brennen. Fundamentals of multiphase flow. 2005.
- [3] S. Chen, S. A. Billings, and P. M. Grant. Non-linear system identification using neural networks. *International Journal of Control*, 51(6):1191–1214, 1990.
- [4] R. González-García, R. Rico-Martínez, and I.G. Kevrekidis. Identification of distributed parameter systems: A neural net based approach. *Computers & Chemical Engineering*, 22:S965–S968, 1998. European Symposium on Computer Aided Process Engineering-8.
- [5] Maziar Raissi, Paris Perdikaris, and George Em Karniadakis. Physics informed deep learning (part ii): Data-driven discovery of nonlinear partial differential equations. *ArXiv*, abs/1711.10566, 2017.
- [6] John H. Lagergren, John T. Nardini, Ruth E. Baker, Matthew J. Simpson, and Kevin B. Flores. Biologically-informed neural networks guide mechanistic modeling from sparse experimental data. *PLoS Computational Biology*, 16, 2020.
- [7] Bethany Lusch, J. Nathan Kutz, and Steven L. Brunton. Deep learning for universal linear embeddings of nonlinear dynamics. *Nature Communications*, 9(1):4950, 2018.
- [8] Pantelis R. Vlachas, Wonmin Byeon, Zhong Y. Wan, Themistoklis P. Sapsis, and Petros Koumoutsakos. Data-driven forecasting of high-dimensional chaotic systems with long short-term memory networks. *Proceedings of the Royal Society A: Mathematical, Physical and Engineering Sciences*, 474(2213):20170844, 2018.
- [9] Tong Qin, Kailiang Wu, and Dongbin Xiu. Data driven governing equations approximation using deep neural networks. *Journal of Computational Physics*, 395:620–635, 2019.
- [10] John Harlim, Shixiao W. Jiang, Senwei Liang, and Haizhao Yang. Machine learning for prediction with missing dynamics. *Journal of Computational Physics*, 428:109922, 2021.

Table 13: Best and mean MSE for the Burger's equation with varying coefficients among 5 runs

	GP	SPL	FEX
Best	1.329×10^{-4}	5.916×10^{-5}	1.058×10^{-5}
Mean	1.386×10^{-4}	1.207×10^{-4}	1.169×10^{-5}

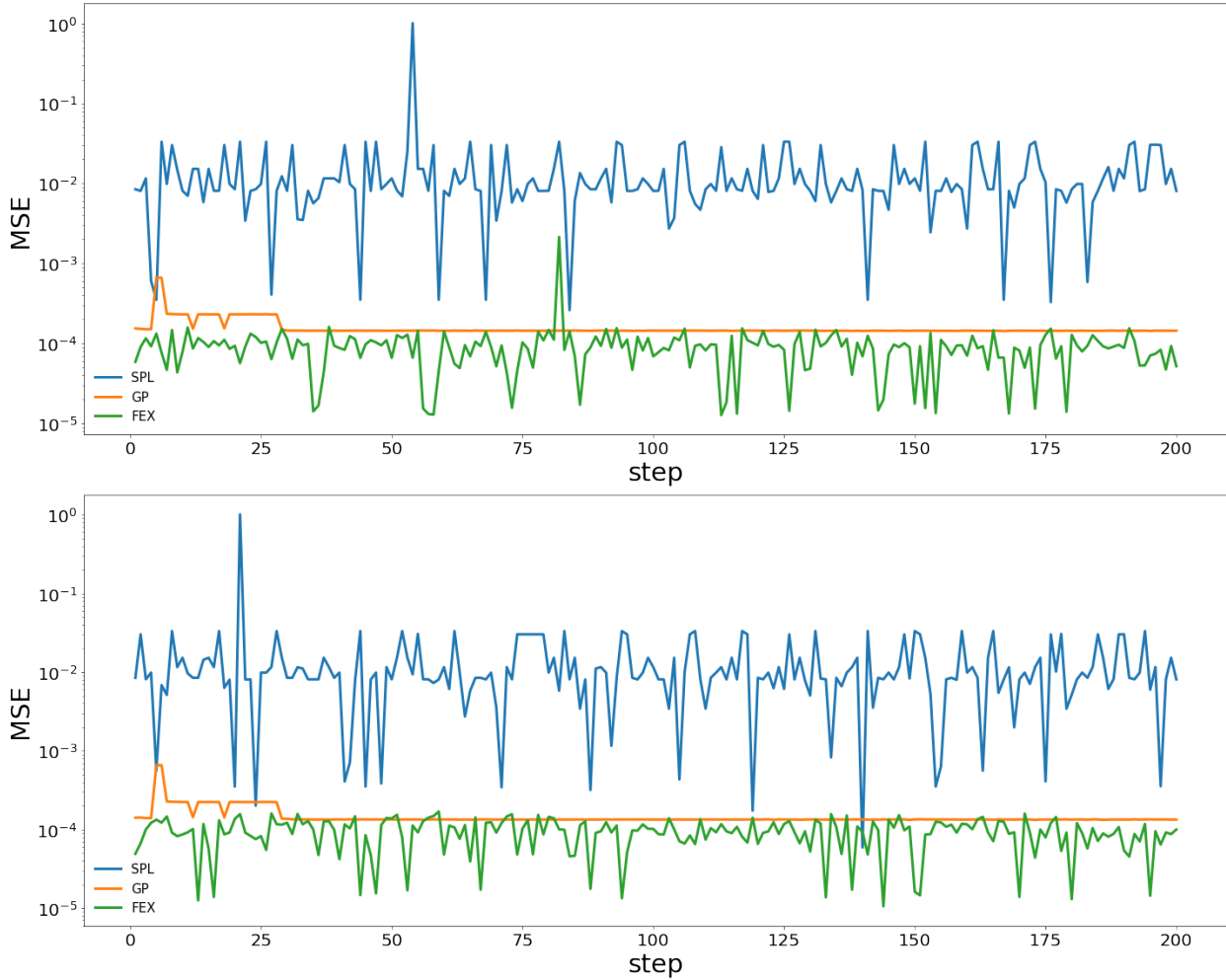


Figure 8: Up: Worst results among 5 runs of three methods. Down: Best results among 5 runs of three methods

- [11] Josh Bongard and Hod Lipson. Automated reverse engineering of nonlinear dynamical systems. *Proceedings of the National Academy of Sciences*, 104(24):9943–9948, 2007.
- [12] Michael Schmidt and Hod Lipson. Distilling free-form natural laws from experimental data. *science*, 324(5923):81–85, 2009.
- [13] Steven L Brunton, Joshua L Proctor, and J Nathan Kutz. Discovering governing equations from data by sparse identification of nonlinear dynamical systems. *Proceedings of the national academy of sciences*, 113(15):3932–3937, 2016.
- [14] Samuel H Rudy, Steven L Brunton, Joshua L Proctor, and J Nathan Kutz. Data-driven discovery of partial differential equations. *Science advances*, 3(4):e1602614, 2017.
- [15] Hayden Schaeffer. Learning partial differential equations via data discovery and sparse optimization. *Proceedings of the Royal Society A: Mathematical, Physical and Engineering Sciences*, 473(2197):20160446, 2017.

Table 14: Comparison for the Avrami equation with different k .

Correct function	$y = 1 - \exp(-kt^2)$
PDE-Net 2.0	$y = 0.2613tk + 0.7284t^2k - 0.2751t^2k^2 \dots$
SINDy	$y = -0.0285tk - 0.0435tk + 1.0385t^2k + \dots$
GP	$y = 0.829kt^2$
SPL	$y = 0.789kt^2$
FEX	$y = 0.9996 - \exp(-0.9997kt^2)$

Table 15: Best and mean MSE for the Burger's equation with varying coefficients among 5 runs

	GP	SPL	FEX
Best	3.936×10^{-5}	1.103×10^{-4}	2.169×10^{-15}
Mean	7.184×10^{-5}	5.329×10^{-4}	1.169×10^{-13}

- [16] Kathleen Champion, Bethany Lusch, J. Nathan Kutz, and Steven L. Brunton. Data-driven discovery of coordinates and governing equations. *Proceedings of the National Academy of Sciences*, 116(45):22445–22451, 2019.
- [17] Zongmin Wu and Ran Zhang. Learning physics by data for the motion of a sphere falling in a non-newtonian fluid. *Communications in Nonlinear Science and Numerical Simulation*, 67:577–593, 2019.
- [18] Hayden Schaeffer, Giang Tran, Rachel Ward, and Linan Zhang. Extracting structured dynamical systems using sparse optimization with very few samples. *Multiscale Modeling & Simulation*, 18(4):1435–1461, 2020.
- [19] Haibin Chang and Dongxiao Zhang. Identification of physical processes via combined data-driven and data-assimilation methods. *Journal of Computational Physics*, 393:337–350, 2019.
- [20] Zhuozhuo Tu, Fengxiang He, and Dacheng Tao. Understanding generalization in recurrent neural networks. In *International Conference on Learning Representations*, 2020.
- [21] Qiang Du, Yiqi Gu, Haizhao Yang, and Chao Zhou. The discovery of dynamics via linear multistep methods and deep learning: Error estimation. *SIAM Journal on Numerical Analysis*, 60(4):2014–2045, 2022.
- [22] Zichao Long, Yiping Lu, and Bin Dong. Pde-net 2.0: Learning pdes from data with a numeric-symbolic hybrid deep network. *Journal of Computational Physics*, 399:108925, 2019.
- [23] Zichao Long, Yiping Lu, Xianzhong Ma, and Bin Dong. Pde-net: Learning pdes from data. In *International Conference on Machine Learning*, pages 3208–3216. PMLR, 2018.
- [24] Stephanie Forrest. Genetic algorithms: principles of natural selection applied to computation. *Science*, 261(5123):872–878, 1993.
- [25] John R Koza. Genetic programming as a means for programming computers by natural selection. *Statistics and computing*, 4:87–112, 1994.
- [26] Yiqun Wang, Nicholas Wagner, and James M Rondinelli. Symbolic regression in materials science. *MRS Communications*, 9(3):793–805, 2019.
- [27] Brenden K Petersen, Mikel Landajuela Larma, Terrell N. Mundhenk, Claudio Prata Santiago, Soo Kyung Kim, and Joanne Taery Kim. Deep symbolic regression: Recovering mathematical expressions from data via risk-seeking policy gradients. In *International Conference on Learning Representations*, 2021.
- [28] Fangzheng Sun, Yang Liu, Jian-Xun Wang, and Hao Sun. Symbolic physics learner: Discovering governing equations via monte carlo tree search. In *The Eleventh International Conference on Learning Representations*, 2023.
- [29] Senwei Liang and Haizhao Yang. Finite expression method for solving high-dimensional partial differential equations. *arXiv preprint arXiv:2206.10121*, 2022.
- [30] Jian-Feng Cai, Bin Dong, Stanley Osher, and Zuowei Shen. Image restoration: total variation, wavelet frames, and beyond. *Journal of the American Mathematical Society*, 25(4):1033–1089, 2012.

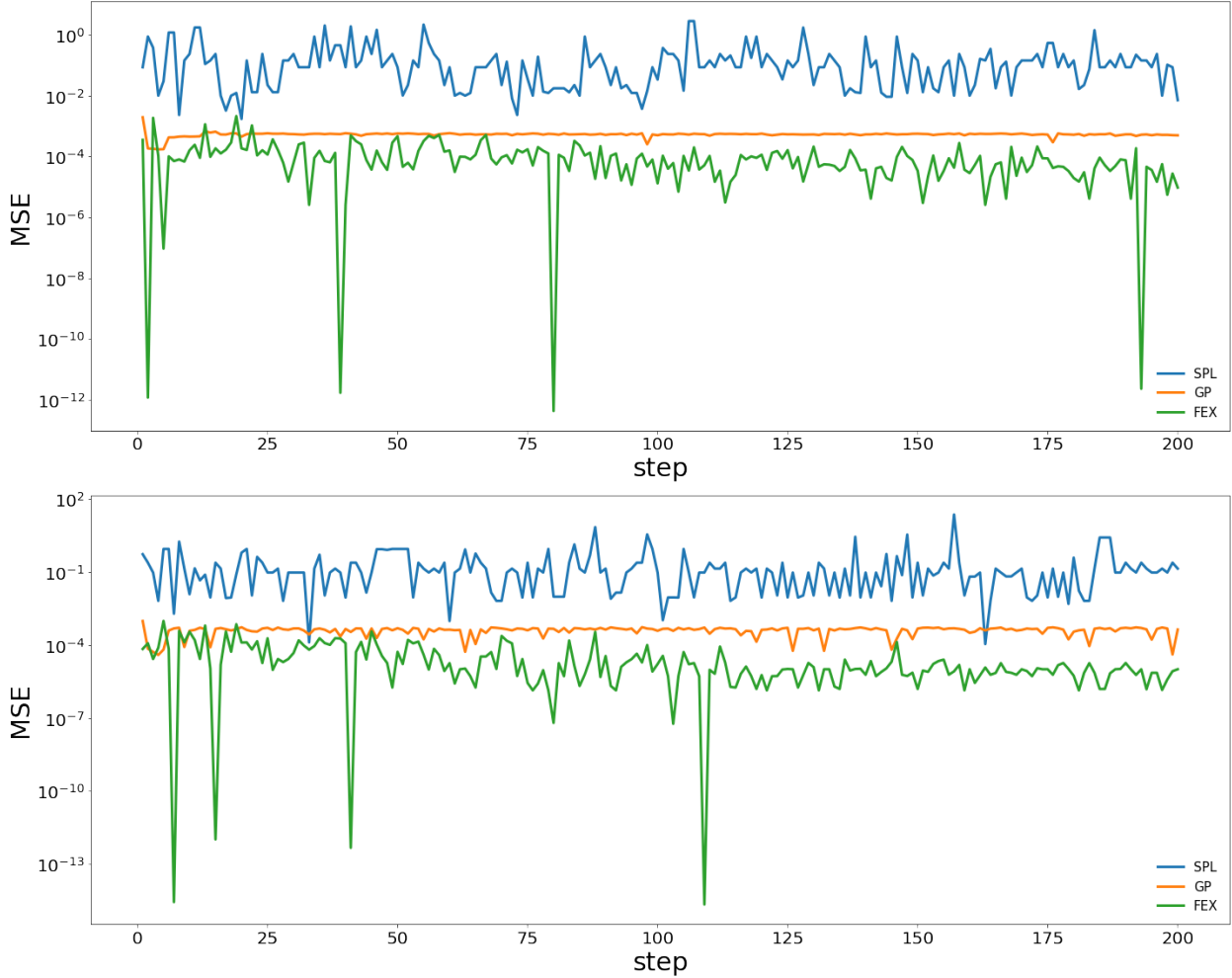


Figure 9: Up: Worst results among 5 runs of three methods. Down: Best results among 5 runs of three methods

- [31] Bin Dong, Qingtang Jiang, and Zuowei Shen. Image restoration: Wavelet frame shrinkage, nonlinear evolution pdes, and beyond. *Multiscale Modeling & Simulation*, 15(1):606–660, 2017.
- [32] David E Rumelhart, Geoffrey E Hinton, and Ronald J Williams. Learning representations by back-propagating errors. *nature*, 323(6088):533–536, 1986.
- [33] Diederik P Kingma and Jimmy Ba. Adam: A method for stochastic optimization. *arXiv preprint arXiv:1412.6980*, 2014.
- [34] Roger Fletcher. *Practical methods of optimization*. John Wiley & Sons, 2013.
- [35] Brenden K Petersen, Mikel Landajuela Larma, T Nathan Mundhenk, Claudio P Santiago, Soo K Kim, and Joanne T Kim. Deep symbolic regression: Recovering mathematical expressions from data via risk-seeking policy gradients. *arXiv preprint arXiv:1912.04871*, 2019.
- [36] Aviv Tamar, Yonatan Glassner, and Shie Mannor. Policy gradients beyond expectations: Conditional value-at-risk. *arXiv preprint arXiv:1404.3862*, 2014.
- [37] Aoxue Chen and Guang Lin. Robust data-driven discovery of partial differential equations with time-dependent coefficients. *arXiv preprint arXiv:2102.01432*, 2021.
- [38] Yingtao Luo, Qiang Liu, Yuntian Chen, Wenbo Hu, and Jun Zhu. Ko-pde: Kernel optimized discovery of partial differential equations with varying coefficients. *arXiv e-prints*, pages arXiv–2106, 2021.
- [39] Samuel Rudy, Alessandro Alla, Steven L Brunton, and J Nathan Kutz. Data-driven identification of parametric partial differential equations. *SIAM Journal on Applied Dynamical Systems*, 18(2):643–660, 2019.